Relationship between Receptor/Ligand Binding Affinity and Adhesion Strength

Suzanne C. Kuo and Douglas A. Lauffenburger
Department of Chemical Engineering, University of Illinois at Urbana-Champaign, Urbana, IL 61801 USA

ABSTRACT Receptor-mediated cell adhesion is a central phenomenon in many physiological and biotechnological processes. Mechanical strength of adhesion is generally presumed to be related to chemical affinity of receptor/ligand bonds, but no experimental study has been previously directed toward this issue. Here we investigate the dependence of receptor/ligand adhesion strength on bond affinity using a radial fluid flow chamber assay to measure the force needed to detach polystyrene beads covalently coated with immunoglobulin G from glass surfaces covalently coated with protein A. A spectrum of animal species sources for immunoglobulin G permits examination of three decades of protein A/immunoglobulin G binding affinity. Our results for this model system demonstrate that adhesion strength varies with the logarithm of the binding affinity, consistent with a prediction from the theoretical model by Dembo et al. (Dembo, M., D. C. Torney, K. Saxman, and D. Hammer. 1988. *Proc. R. Soc. Lond. Ser. B* 234:55–83).

GLOSSARY

A_c	contact area
a	contact area radius
B_i	number of bonds in contact region
C	bound receptor number
f_b	force to break single bond
F_t	total force to detach bead/cell
H	maximum plate and bead separation distance
h	gap width between two disks
h_s	separation distance between plate and bead
k_B	Boltzmann's constant
K_D	equilibrium dissociation constant
L	solution ligand concentration
l_b	extent of stretch to reach f_b
N_b	bond density
N_L	substratum ligand density
N_R	receptor density
Q	volumetric flow rate
r	radial distance from center of chamber
r_c	critical radius
R_T	receptor number per bead
R_c	receptor number per bead in contact region
S	surface shear stress
S_c	critical shear stress
T_{crit}	critical tension on sphere
α	front angle between membrane and surface
γ	adhesion energy
μ	fluid viscosity
η	conversion parameter for K_D
ρ_B	bead radius
θ	temperature

INTRODUCTION

Receptor-mediated cell adhesion plays a crucial role in many physiological and biotechnological processes. For example, leukocyte and tumor cell homing to particular tissues is accomplished by specific receptor interactions with endothelial ligands (Springer, 1990). Also, cell affinity chromatography can be used for depletion of tumor cells from bone marrow for autologous transplantation, enrichment of stem cells from the bone marrow for allogeneic transplantation or for gene therapy, and isolation of fetal cells from maternal blood for genetic diagnosis (Berenson et al., 1986; Sharma and Mahendroo, 1980).

A long-standing issue in cell adhesion is how receptor-mediated cell/cell or cell/substratum adhesion strength is related to receptor/ligand binding affinity. While models for a variety of cell behavior involving receptor-mediated adhesion invoke a connection between these two quantities (Bell et al., 1984; Hammer and Lauffenburger, 1987; Dembo et al., 1988; DiMilla et al., 1991), no direct experimental test has been heretofore conducted. Information on this relationship should be useful as a guide to molecular design in applications as diverse as cell separations, biomaterials, cell and developmental biology, and tissue engineering. We provide in this paper the first experimental investigation directed toward this issue.

Because we desire to focus on receptor/ligand interactions as purely as possible, we have chosen to use protein-coated 10-μm diameter latex polystyrene microspheres as "model" cells. These beads serve our purposes particularly well for five reasons: (a) types and numbers of "receptors" can be systematically varied; (b) complicating features associated with real cells, such as membrane diffusion, cell viscoelastic deformation behavior, and receptor/cytoskeletal interactions, are absent; (c) covalent linkage of protein "receptors" to the beads by carbodiimide chemistry, as well as of protein "ligands" to substrata via silane coupling techniques, reduces ambiguity regarding the mode of bond disruption; (d) comparative nondeformability of the beads allows a constant bead/substratum contact area; and (e) relatively smooth bead surface permits reasonable estimation of the contact area. Although we do not claim immediate correspondence of the data we obtain with our model cells to observations on real

Received for publication 20 January 1993 and in final form 9 August 1993.
Address reprint requests to Douglas A. Lauffenburger, Department of Chemical Engineering, 114 Roger Adams Laboratory, University of Illinois at Urbana-Champaign, 600 S. Mathews Avenue, Urbana, IL 61801.

0006-3495/93/11/2191/10 $2.00

cells, because of the obvious simplifications, we believe that important insights can be gained into biophysical characteristics of the underlying receptor/ligand interactions.

Animal immunoglobulin G (IgG) antibodies were chosen for the receptor linked to the bead surface. Protein A (SpA), a cell-wall constituent of *Staphylococcus aureus*, was chosen as the complementary ligand. Protein A specifically binds the Fc region of immunoglobulins, mainly IgG, from different mammalian species (Langone, 1982a). SpA/IgG provides a useful receptor/ligand system because of its well-studied binding interactions and potential for alteration of binding affinity (as well as rate constants) by available methods (Langone, 1982a,b; Pharmacia, 1992).

Adhesion strength was determined from measurement of the critical shear stress for detachment of beads from the coated glass substratum in the radial fluid flow chamber, following Cozens-Roberts et al. (1990). This device is well suited for these studies because a range of fluid shear stresses can be applied in a single experiment, with the linear fluid velocity decreasing reciprocally as radial distance from the fluid inlet increases in the chamber. Shear stress values can be converted to total force using an analysis of the translational force and rotational torque for a spherical particle near a surface (Hammer and Lauffenburger, 1987; Goldman et al., 1967).

We varied the receptor/ligand binding affinity by two separate means: alteration of the pH of the fluid medium and use of IgG antibodies from different animal species. Binding parameters (receptor number and equilibrium dissociation constant, K_D) were measured by fluorescence flow cytometry using fluorescein-labeled SpA in solution binding to IgG-coated beads. Total substratum ligand density was measured by determining radioactivity levels of substratum coated with ^{125}I-labeled SpA, and functional ligand density was determined by using ^{125}I-labeled antibodies binding to SpA-coated glass plates. The contact area was estimated from geometric considerations (Cozens-Roberts et al., 1990).

Our experimental results were analyzed in terms of an existing theoretical model for cell adhesion by Dembo et al. (1988). Combined with an expression for adhesion energy density by Evans (1985), this model successfully describes our data, which show a logarithmic dependence of mechanical detachment force on chemical affinity.

MATERIALS AND METHODS

Radial-flow detachment assay

The radial-flow detachment assay (RFDA) is a procedure that conveniently measures the strength of adhesion between a particle and a surface (Cozens-Roberts et al., 1990). Fluid flow in a radial direction between two parallel surfaces within the chamber provides a shear force capable of detaching "receptor"-coated particles initially adhered to a "ligand"-coated glass disc. Since the fluid dynamics within the chamber are well characterized, the particle/surface adhesion strength can be determined from the shear force needed for detachment under any particular conditions.

The apparatus consists of a chamber, a ligand-coated disc, a fluid source (separatory funnel), and the microscope system. A schematic diagram of the cross-section of the radial-flow detachment chamber is shown in Fig. 1. The

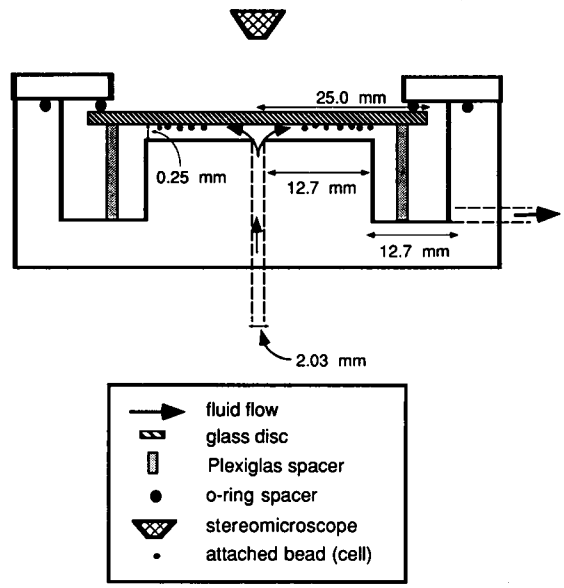

FIGURE 1 Schematic cross-section diagram of the radial-flow detachment chamber. Fluid flow in a radial direction between two parallel surfaces provides the shear force capable of detaching receptor-coated model cells from the ligand-coated glass disc (Cozens-Roberts et al., 1990). The surface shear stress decreases with increasing radial position, allowing the particle/surface adhesion strength to be determined.

ligand-coated, 50-mm diameter, flat glass disc is placed in the Plexiglas chamber above a 25.4-mm diameter cylinder. The separation between these two flat surfaces is 0.254 mm, maintained with three Plexiglas spacers. Fluid flows radially through this gap, detaching beads bound to the glass disc. The surface shear stress, S, decreases radially with distance from the center of the chamber. From fluid flow calculations, the shear is inversely proportional to the radius. Therefore, beads will be detached in the region near the center of the chamber (higher shear stresses) and the beads will remain adhered in the outer radii (lower shear stresses). Direct observation of the number of beads attached before and after flow of buffer can be made through a Carl Zeiss (Batavia, IL) SV8 stereomicroscope. These quantities provide information on the strength of adhesion.

Receptor-coated beads injected into the chamber are allowed to incubate for a period of 30 min, and the surface is scanned along the x and y axes to count initially adhered beads. Constant buffer flow is then applied for 30 min until a stable critical radius develops. The remaining adherent beads are counted along the same axes, and the percentage remaining can then be determined as a function of radial position, r. A boundary exists where fluid flow has detached all beads between the center entrance port and the region where beads remain attached. This critical radius, r_c, marks where the force and torque of the fluid on the particle are exactly counteracted by the bead's adhesive stresses in the cell-substrate interface. By convention, we define r_c to be the radius where the adherent percentage after flow begins to deviate from 0%. We can calculate the shear stress present at any radius with the expression (Cozens-Roberts et al., 1990):

$$S = \frac{3Q\mu}{\pi r h^2} \quad (1)$$

where Q is the volumetric flow rate, μ is the fluid viscosity, r is the radius, and h is the gap width between the two discs. From a plot of percentage bound after flow versus shear stress, a critical shear stress, S_c, can be determined from the radius where the beads just begin to remain attached.

Receptor and ligand

Animal IgG antibodies were used as the bead receptors. The antibodies tested were rabbit, mouse, pig, goat, and sheep. Rabbit and mouse polyclonal, chromatographically purified IgG antibodies were purchased in

buffer solution from Zymed Laboratories (South San Francisco, CA). Pig, goat, and sheep polyclonal antibodies were purchased from Sigma Immunochemicals (St. Louis, MO).

The ligand chosen was recombinant SpA from *Escherichia coli*, purchased from Zymed Laboratories in lyophilized powder form. The protein was prepared from the cytosol of an *E. coli* strain containing the gene for SpA from *S. aureus* Cowan I strain.

SpA conjugated with fluorescein isothiocyanate was also purchased from Zymed Laboratories. SpA was radiolabeled with ^{125}I using IODO-Beads iodination reagent purchased from Pierce (Rockford, IL), following Markwell (1982). Binding more than one ^{125}I atom per protein A molecule via tyrosine residues can impair the molecule's ability to bind IgG (Markwell, 1982), so a low transfer efficiency of ^{125}I was desired. ^{125}I was purchased from DuPont (Wilmington, DE) as $Na^{125}I$ in solution. Iodination was performed with a single IODO-Bead and 1.0 mCi of ^{125}I. The bead was incubated for 15 min with 100 μg of protein. By using a large amount of protein, a lower efficiency of incorporation was obtained. Separation of the free iodine from the protein was carried out on a Sephadex G-10 column. Fractions were taken and counts measured on a Cobra Auto-Gamma Counting System, model B5002 (Packard Instrument Company, Meriden, CT).

Fluorescence measurements were made on an EPICS model 752 flow cytometer (Coulter Electronics, Hialeah, FL) equipped with an Innova 90–5 argon ion laser (Coherent, Palo Alto, CA). The water-cooled laser was tuned to 488 nm with a sample laser power of about 350 mW. Fluorescence histograms were collected based on gated bit maps of forward angle light scatter versus 90° light scatter. A 515 nm long-pass filter was used in front of the photomultiplier tube collecting fluorescence signals. A dichroic 488 nm long-pass filter in front of the photomultiplier tube collected 90° light scatter. A third photomultiplier tube collected forward angle light scatter with a gain of 10. The voltages were adjusted to increase the sensitivity, keeping both the lowest and the highest fluorescent samples on the three-decade log scale. A Coulter Multiparameter Data Acquisition and Display System was used to display, analyze, and store data.

Experiments involving ^{125}I-labeled SpA were performed to determine receptor number and SpA densities on the bead and plate surfaces, respectively. Actual functional receptor/ligand binding sites were also measured using ^{125}I-labeled antibodies. In addition, radiolabeled equilibrium experiments were used to obtain calibration ratios for conversion of flow cytometry data to exact numbers of proteins. Details can be found in Kuo (1992).

Plate and bead coating

Polystyrene latex microspheres $(C_8H_8)_n$ were purchased as carboxylated microspheres, 2.5% suspension, from Polysciences, Inc. (Warrington, PA) and were reported by that company to have an average diameter of 10 μm as determined by the centrifuge assay. However, Coulter Counter and flow cytometry analysis performed in our laboratory discovered a biphasic population of beads, with 70% of the beads having an 8-μm diameter and 30% with a 10-μm diameter. Both subpopulations exhibited small variance relative to their means. All experiments were carried out with this particular lot of beads, and thus calculations are adjusted for this bead size distribution.

Carbodiimide chemistry was used to covalently link the protein, IgG, to activated carboxylate groups on the bead surface. Water-soluble carbodiimide (ethyl-3-(3-dimethylamino)propyl carbodiimide, $C_8H_{18}ClN_3$) can couple compounds containing functional groups, such as amines and carboxylic acids (Goodfriend et al., 1964). The carbodiimide links the protein amine groups to the activated carboxylate groups on the surface of the bead. The chemicals and coating procedure were supplied in a carbodiimide kit from Polysciences, Inc. The coating procedure involved preparation of the carboxylate bead surface by washing sequentially in carbonate and phosphate buffer solutions. A 2% solution of carbodiimide in phosphate buffer was added to the beads and mixed for 3–4 h. After the unreacted carbodiimide was removed by washes with borate buffer, the protein was added in amounts ranging from 20 to 200 μg. After an overnight incubation, ethanolamine was added to block unreacted sites, and bovine serum albumin served to block any remaining nonspecific binding sites. Details of the coating procedure can be found in Cozens-Roberts et al. (1990) and Kuo (1992).

Optical round flat glass discs (50-mm diameter, 3-mm thickness) were used as the protein-coated surfaces in the chamber. The discs were purchased from Melles Griot (Irvine, CA). The discs were vigorously cleaned by soaking in concentrated nitric acid for 15 min, rinsing in deionized water, and soaking in 4 mM NaOH. After overnight drying, the discs were then silanized by soaking in a solution of 2% v/v 3-aminopropyltriethoxysilane (Sigma, St. Louis, MO) in acetone under constant agitation for 10 min. This procedure covalently couples 3-aminopropyltriethoxysilane to the glass while forming an alkylamine carrier (Weetal, 1976), creating a hydrophobic surface onto which glutaraldehyde can couple. Glutaraldehyde was purchased as 8.0% in treated water from Eastman Kodak (Rochester, NY). A glutaraldehyde solution of 1.1% v/v in treated water was prepared immediately before use. A volume of 5.0 ml of the glutaraldehyde solution was placed on the surface of each disc and allowed to incubate for 30 min at room temperature. The disc then became an aldehyde carrier to which a ligand can be covalently coupled via an amine group to the aldehyde group (Weetal, 1976). A 5.0-ml solution of SpA at a concentration of 50 μg/ml was then incubated with the surface for 2 h creating a hydrophilic surface. Finally, the discs were rinsed in treated water and soaked in 5.0 ml of 0.2 M glycine to bind any remaining aldehyde groups on the glass surface. Discs were stored up to 3 days in phosphate-buffered saline (PBS), containing 0.1% sodium azide and 1.0% bovine serum albumin.

Protein quantitation

Total receptor number on the beads was determined using flow cytometry. The beads were incubated for 30 min with a saturating amount of fluorescent SpA. In addition, beads without IgG, but treated similarly as the beads in the coating steps, were incubated with fluorescent SpA as controls. Samples were analyzed with the flow cytometer and fluorescent signals were converted to the number of SpA molecules bound to each bead. Concentration of the beads in the sample was measured by Coulter Counter model ZM (Coulter Electronics).

A calibration ratio was needed to convert flow cytometry results to actual number of protein molecules bound to the surface. To determine this effective calibration ratio, equilibrium binding experiments with ^{125}I-labeled SpA were performed and compared with the fluorescence signals obtained with the flow cytometer.

The glass coating procedure was repeated using ^{125}I-labeled SpA diluted with cold protein A to determine the total SpA coating density. A glass disc used for the RFDA experiments was cut into rectangular pieces, which could be placed in the 1-cm gamma counter sample tubes. All steps of the coating procedure were scaled down in volume to the surface areas of the rectangular glass pieces from the surface area of the 50-mm diameter discs. The coating procedure of SpA at the same solution concentration was performed and the radioactive signal was measured on the gamma counter. We determined the total SpA density to be $3.5 \times 10^{12} \pm 0.5 \times 10^{12}$ #/cm^2. This represents the total protein on the surface, rather than the functional protein.

The density of active binding sites on SpA was determined by first coating glass plates with unlabeled SpA and then saturating the binding sites with radiolabeled antibodies. The density of bound antibodies can then be compared for different species or pH conditions to determine if the number of functional sites varies. Rabbit IgG (Zymed Laboratories) was radiolabeled with ^{125}I using IODO-Beads iodination reagent. Radiolabeled ^{125}I-mouse IgG antibody was purchased from ICN Biomedicals, Inc. (Irvine, CA). The glass plates were first coated with SpA at a concentration of 50 μg/ml. Then, a saturating amount of radiolabeled antibody (50 μg/ml), diluted in cold antibody, was incubated on the top surface of the glass plate. Antibodies tested were rabbit and mouse, in PBS buffer, pH 7.4. In addition, rabbit IgG in pH 3.0 PBS buffer was used. After incubation of the antibody with the surface for 20 min and a quick wash step with buffer, the radioactive signal was measured on the gamma counter, and the amount of bound antibody was calculated.

Flow cytometry

Quantum 26 calibration beads were purchased from Flow Cytometry Standards Corporation (Research Triangle Park, NC). These standards allow for

a direct correlation between the fluorescence signal obtained on the flow cytometer (channel number) with a quantity referred to as Molecules of Equivalent Soluble Fluorochrome (MESF). MESF units were determined by comparing the fluorescence signal from the calibration beads to the signal from a solution of the same fluorochrome. MESF units give a measure of the intensity relative to a solution, not the actual number of fluorochrome molecules.

Equilibrium binding data were collected by incubating a range of concentrations of fluorescent SpA with the beads and measuring the fluorescent signal on the flow cytometer. Concentration of fluorescent SpA ranged from 0 to 125 μg/ml. Control beads were also incubated with equivalent amounts and concentrations of fluorescent SpA. The beads were incubated for 30 min at room temperature, and the fluorescence intensities were measured on the flow cytometer. The mean channel of each fluorescence histogram was determined and converted to number of bound fluorescent SpA molecules, using the MESF/protein ratio.

Estimation of contact area

The area of the contact region for a smooth, relatively nondeformable particle can be estimated using geometrical considerations (Cozens-Roberts et al., 1990). A schematic diagram of a bead in contact with a surface is shown in Fig. 2 (not drawn to scale). The contact region can be defined as that permitting approach of bead and glass surfaces to within about 40 nm. The minimum separation distance between the plate and bead, h_s, and the maximum separation distance for receptor/ligand binding, H, are assigned values of 10 and 40 nm, respectively, based on approximate dimensions of IgG and protein A. Calculations using these values yielded values for the contact region radius, a, of 0.40 and 0.45 μm for 8- and 10-μm diameter beads, respectively, corresponding to roughly 10% of the original bead radii. The order of magnitude of this estimate has been experimentally validated, albeit in approximate fashion, using interference reflection microscopy (Saterbak et al., 1993). The contact area, then, takes on a value between πa^2 and $2\pi a^2$, depending on the extent of curvature; we consider this factor of 2 to be within our level of uncertainty.

Buffer pH experiments

Initial experiments involved altering the fluid medium pH to observe variations in adhesion strength with binding affinity. Polyclonal, chromatographically purified rabbit anti-goat IgG (Zymed Laboratories) and goat IgG (Sigma Immunochemicals) were covalently coupled to the beads and glass via free amine groups using carbodiimide and glutaraldehyde chemistry, respectively. PBS over a range of pH (5–9) was used as the fluid medium.

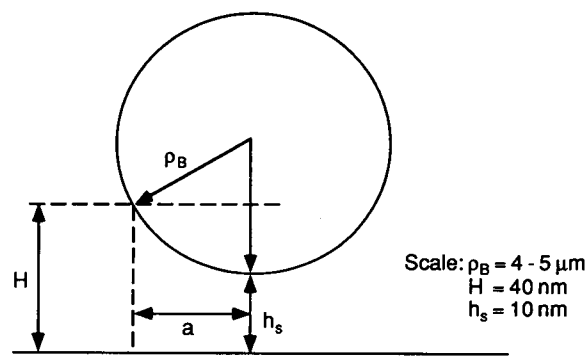

FIGURE 2 Schematic diagram showing geometrical determination of contact area of a nondeformable bead with a surface, where h_s is the separation distance between surfaces, H is the maximum separation, ρ_B is the radius of the bead, and a is the radius of the contact area (Cozens-Roberts et al., 1990). Specifying h_s = 10 nm and H = 40 nm, the contact area radius, a, is calculated to be approximately 10% of the bead radius, ρ_B, for 8- and 10-μm diameter beads.

Critical detachment stress, S_c, as a function of pH, was previously obtained by Cozens-Roberts et al. (1990). Using fluorescence flow cytometry, we determined K_D from equilibrium binding of fluorescent ligand in solution to receptor-coated beads in the same pH buffer solutions. Fluorescein-labeled goat IgG in PBS was incubated over a range of concentrations with rabbit anti-goat IgG-coated beads for 30 min. K_D values, along with total receptor number per bead, R_T, were found by fitting data on receptor/ligand complex number, C, versus solution ligand concentration, L, to the equilibrium binding expression: $C = R_T \times L/(K_D + L)$. S_c and K_D were both measured for a series of fluid medium pH values, which were adjusted by using appropriate HCl and NaOH solutions.

RESULTS

An initial set of experiments was performed to see whether a previously observed variation of adhesion strength with fluid medium pH, using goat IgG antibodies as the substratum ligand on the glass and rabbit anti-goat IgG antibodies as the cell receptors on the beads, could be accounted for by corresponding variation in goat/rabbit anti-goat binding affinity. Fig. 3 shows data for the critical detachment stress, S_c, as a function of pH, previously obtained by Cozens-Roberts et al. (1990). S_c decreases from a maximal value as pH is raised or lowered from a physiological value of 7.4. To learn whether bond affinity changes might be responsible for this effect, we measured the equilibrium dissociation constant, K_D, for this receptor/ligand pair for the same pH values. These data are also plotted in Fig. 3 for comparison. Increases in K_D as pH is raised or lowered from 7.4 are qualitatively associated with the decreases in S_c. Therefore, adhesion strength correlates directly with measured bond affinity, the reciprocal of K_D. This represents a first experimental observation demonstrating a relationship between the two quantities.

However, it is necessary to know what portion of the adhesion strength is due to "specific" receptor/ligand bond

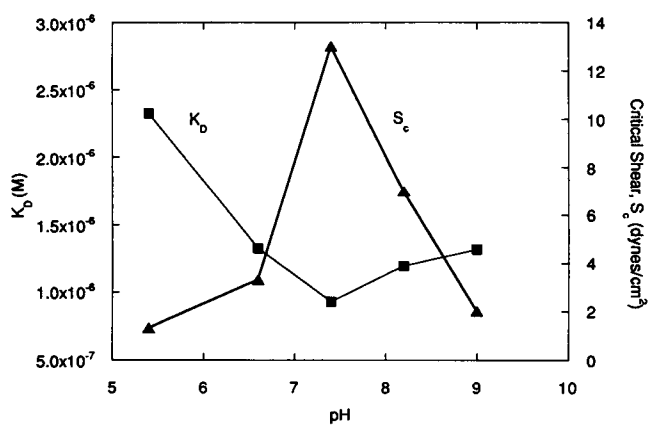

FIGURE 3 Critical shear stress, S_c, for detachment of beads coated with rabbit anti-goat IgG from goat IgG-coated glass in the radial flow chamber (reproduced from Cozens-Roberts et al., 1990) and equilibrium dissociation constant, K_D, versus fluid medium pH (present work). In these earlier experiments, S_c was determined from the radial position, r_c, in the flow chamber at which 50% of the initially deposited beads were detached by 30 min of shear flow, using Eq. 1. K_D was determined from equilibrium binding of fluorescent ligand in solution to receptor-coated beads using flow cytometry.

forces in contrast to "nonspecific" colloidal forces between protein-coated surfaces. This can be determined by measuring the critical detachment stress as a function of cell receptor number. The slope of this function should primarily characterize the specific bond forces whereas the intercept should give the nonspecific forces in the absence of any bonds (Cozens-Roberts et al., 1990). We thus applied this approach, but now focused our effort on the IgG/SpA receptor/ligand pair.

We first changed IgG/SpA binding affinity by altering medium pH. Fig. 4 shows detachment stress data as a function of the number of IgG molecules on the beads, for pH = 7.4 and 3.0, with rabbit IgG and SpA. The slope of the curve for pH = 3.0 is lower than that for pH = 7.4, indicating a smaller specific adhesion strength. The intercept is slightly greater at the lower pH, implying a larger nonspecific attraction. This may arise from changes in protein and surface charges as pH is altered. However, control experiments in which ionic strength was varied yielded no significant effects on detachment stress.

The key quantitative result of Fig. 4 is that the slope, or, the specific adhesion strength, on a per receptor basis, is diminished by a factor of 2.3 by the pH change from 7.4 to 3.0. How does this compare to a measured change in bond affinity? Fig. 5 shows comparative equilibrium binding data for these two pH levels. Averages of three such experiments yielded K_D values of 4.6×10^{-9} and 1.8×10^{-7} M for pH = 7.4 and 3.0, respectively. Bond affinity is thus decreased by a factor of 30 for pH = 3.0 relative to 7.4. Transient binding experiments showed that this decrease was primarily due to a large drop in the association rate constant at the lower pH (Kuo, 1992).

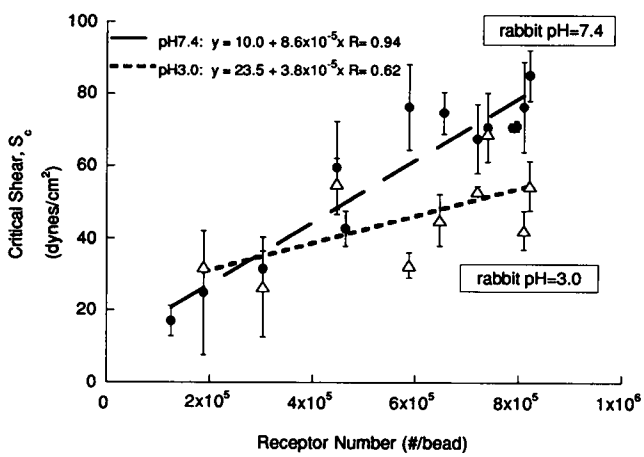

FIGURE 4 Critical shear stress, S_c, for detachment of beads coated with rabbit IgG from SpA-coated glass in the radial-flow chamber, comparing pH = 7.4 and 3.0. The number of IgG molecules on the beads was varied. Slopes represent specific adhesion force mediated by receptor/ligand bonds, while ordinate intercepts represent nonspecific adhesion force occurring in the absence of receptor/ligand bonds (Cozens-Roberts et al., 1990). For pH = 7.4, the slope is $8.6 \times 10^{-5} \pm 0.9 \times 10^{-5}$ (dynes/cm²)/(#/bead); for pH = 3.0 it is $3.8 \times 10^{-5} \pm 1.8 \times 10^{-5}$ (dynes/cm²)/(#/bead), a factor of 2.3 lower than the slope at pH 7.4.

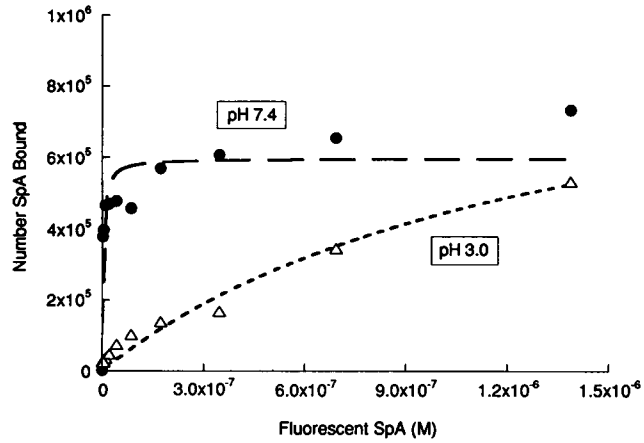

FIGURE 5 Equilibrium binding of fluorescein-labeled SpA in solution to rabbit IgG-coated beads using fluorescence flow cytometry, comparing pH = 7.4 and 3.0, as a function of SpA concentration. Values of the equilibrium dissociation constant, K_D, were obtained as means of three separate experiments for each pH (see Table 1), yielding K_D values of 4.6×10^{-9} M and 1.8×10^{-7} M for pH = 7.4 and 3.0, respectively. Bond affinity is thus decreased by a factor of 30 for pH = 3.0 relative to 7.4.

A more direct approach to altering bond affinity was used to confirm and extend this result. IgG antibodies from different animal species are known to possess different affinities for SpA, rabbit having among the greatest (Langone, 1982a,b) We substituted other animal species IgG for the rabbit IgG as the cell receptors, i.e., the protein immobilized on the beads, keeping the medium pH constant at 7.4 for all species. Experiments were performed for IgG from pig, mouse, sheep, and goat species. Equilibrium binding data were obtained for the various species from fluorescent flow cytometry or literature reports (Langone, 1982b), and values of K_D are listed in Table 1.

As an example, mouse IgG has an affinity for SpA that is approximately 35 times lower than rabbit IgG. Fig. 6 shows corresponding data for critical detachment stress of beads coated with the mouse IgG, compared to an extrapolation of the rabbit IgG data. As before, the beads carrying the lower affinity receptors exhibit a weaker specific adhesion strength. For mouse, in comparison to rabbit, the decrease in slope is now 4.1. Hence, in two different cases, receptor-mediated adhesion strength is decreased by a factor of about 2–4 when binding affinity is decreased by a factor of 30–35, *independent of the means used to change the affinity.*

TABLE 1 Equilibrium binding data for IgG from various species*

Receptor	pH	K_D (M)
Rabbit IgG	7.4	$4.6 \times 10^{-9} \pm 1.7 \times 10^{-9}$
Rabbit IgG	3.0	$1.8 \times 10^{-7} \pm 0.5 \times 10^{-7}$
Mouse IgG	7.4	$1.6 \times 10^{-7} \pm 0.8 \times 10^{-7}$
Pig IgG	7.4	$1.6 \times 10^{-8} \pm 1.0 \times 10^{-8}$
Sheep IgG	7.4	3.1×10^{-6}
Goat IgG	7.4	7.7×10^{-6}

* Equilibrium binding data for various species IgG, obtained from fluorescent flow cytometry experiments (rabbit, mouse, and pig) or literature reports (sheep and goat) (Langone, 1982b).

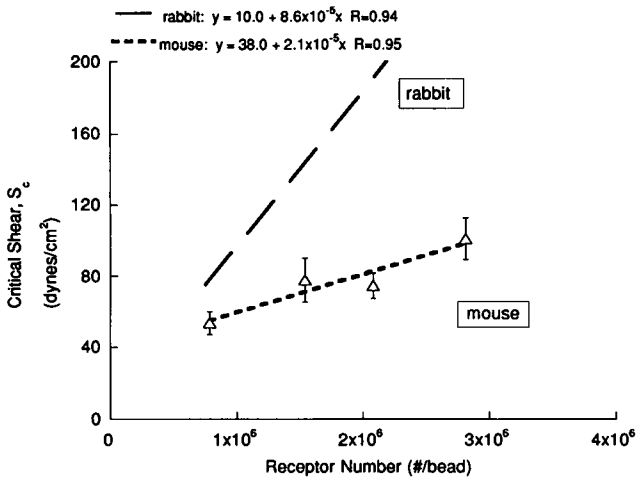

FIGURE 6 Critical shear stress, S_c, for detachment of beads coated with IgG from SpA-coated glass in the radial flow chamber, comparing mouse IgG and rabbit IgG, both at pH = 7.4. Slopes represent specific adhesion force mediated by receptor/ligand bonds, while ordinate intercepts represent nonspecific adhesion force occurring in absence of receptor/ligand bonds (Cozens-Roberts et al., 1990). For mouse IgG, the slope is $2.1 \times 10^{-5} \pm 0.5 \times 10^{-5}$ (dynes/cm^2)/(#/bead); for rabbit IgG the slope (extrapolated from the data in Fig. 4) is $8.6 \times 10^{-5} \pm 0.9 \times 10^{-5}$ (dynes/cm^2)/(#/bead). For mouse, the decrease in slope is a factor of 4.1 relative to rabbit.

We then proceeded to measure the critical detachment stress for each of the IgG species, again as functions of bead receptor number. Fig. 7 shows the slopes of such plots as a function of the K_D values for the various species. Qualitatively, a relationship exists between the slope and the dissociation constant over three decades of K_D values. A larger slope, or greater adhesion strength, corresponds to a smaller dissociation constant, or greater bond affinity.

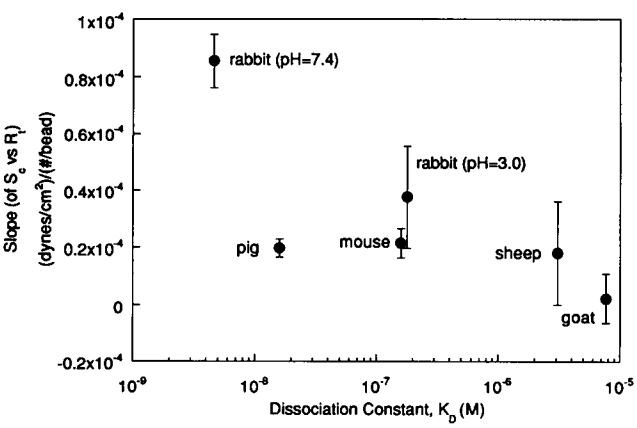

FIGURE 7 Slopes from plots of critical shear stress S_c versus R_T, for detachment of beads coated with IgG from SpA-coated glass in the radial-flow chamber, shown as a function of the dissociation constant (K_D). The measured dissociation constants for the various animal species IgG for solution SpA span 4 decades of the logarithmic scale. Statistical analysis using Spearman's or Kendall's rank correlation shows that the null hypothesis (no association between x and y variables) can be rejected with 96% confidence.

ANALYSIS

As a first step in interpretation of these data, we must convert the critical detachment stress, S_c, to an overall bead/surface adhesion strength. This can be accomplished using the fluid mechanical analysis by Goldman et al. (1967) as applied by Hammer and Lauffenburger (1987). The slopes of the plots of critical detachment stress versus bead receptor number can be multiplied by a conversion factor combining the translational and rotational forces that act on the bead due to the fluid shear stress. In the present case this factor is $110\rho_B^3/a$ (Cozens-Roberts et al., 1990), where a is the radius of the contact region and ρ_B is the bead radius. The forces calculated for 10- and 8-μm beads are determined separately and then added in the appropriate ratio (30 and 70%, respectively) to obtain the overall force required for detachment. We define this quantity as the bead/surface adhesion strength. Using our estimated value for the contact radius of approximately 10% of the bead radius, the adhesion strength per receptor present in the contact region can be calculated, assuming uniform receptor density. This result is displayed in Fig. 8.

In this form, our adhesion strength data can be analyzed in terms of a theoretical treatment previously offered by Dembo et al. (1988). The model is derived from a mechanical force balance on a peeling interface, allowing for stress distribution within the contact region with the greatest stress acting on bonds at the perimeter of the region. The treatment

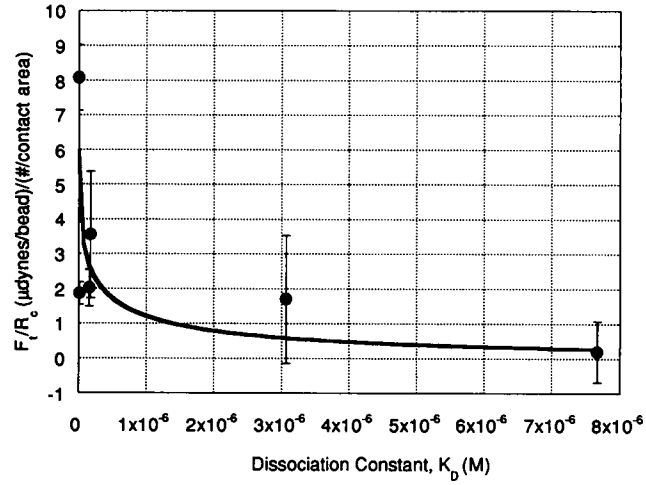

FIGURE 8 Adhesion strength per receptor present in the contact region (F_t/R_c) for the various animal species IgG, as a function of the dissociation constant. The adhesion strengths were calculated by multiplying the slopes of the plots of critical detachment stress versus bead receptor number (Fig. 7) by a conversion factor $110\rho_B^3/a$ (Cozens-Roberts et al., 1990), combining the translational and rotational forces acting on the bead due to the fluid shear stress. The averaged force for the mixed bead population is shown. A weighted least-squares curve fit of the Dembo/Evans expression for the average bond strength, modified by the parameter η as in Eq. 6, to the data specifies $\eta = 1.3 \times 10^{18}$ #-liter/cm^2-mol and $l_b = 8.8$ Å. An average ligand density of 3.5×10^{15} #/cm^2 was used. The fit is characterized by $\chi^2 = 15.7$ and $R = 0.76$.

specifies that the bond association and dissociation rate constants may be altered by input of energy, by a strain-dependent phenomenon.

Dembo et al. define the critical tension T_{crit} as the value required to just begin peeling of a cell surface from the adhesion substratum. A mechanical force balance leads to an expression for T_{crit}:

$$T_{crit} = \frac{k_B \theta N_R \ln\left\{1 + \frac{N_L}{K_D}\right\}}{1 + \cos\alpha} \tag{2}$$

where k_B is Boltzmann's constant, θ is absolute temperature, N_L is the substratum ligand density, α is the front angle between the membrane and the surface, and N_R is the cell receptor density. Equation 2 has the same form as the classical Young equation (Adamson, 1982), and thus the surface energy for bonding between the membrane and the surface is equal to the numerator on the right-hand side of the equation (Dembo et al., 1988):

$$\gamma = k_B \theta N_R \ln\left\{1 + \frac{N_L}{K_D}\right\} \tag{3}$$

Evans (1985) shows that the adhesion energy can also be written in terms of a specific bond force:

$$\gamma = \frac{N_b f_b l_b}{2} = \left(\frac{F_t}{A_c}\right)\frac{l_b}{2} \tag{4}$$

where N_b is the bond density, f_b is the force to break a bond, l_b is the extent of stretch required to reach the peak force f_b, F_t is the total force to detach a bead/cell from the surface, and A_c is the contact area. The total force is obtained by integrating the product of the bond density and bond force over the contact area. Equating Eqs. 3 and 4 and solving for the force per receptor in the contact region gives:

$$\frac{F_t}{R_c} = \frac{2k_B\theta}{l_b} \ln\left\{1 + \frac{N_L}{K_D}\right\} \tag{5}$$

Our measured values of K_D were obtained for solution ligand binding to surface-bound receptors, because there is presently no method available for determining K_D values when both ligand and receptor are surface-bound. Hence, we must rewrite Eq. 5 in terms of our measured, solution/surface K_D values. We accomplish this by including a parameter, η, to convert the measured K_D values to appropriate surface/surface values:

$$\frac{F_t}{R_c} = \frac{2k_B\theta}{l_b} \ln\left\{1 + \frac{N_L}{\eta K_D}\right\} \tag{6}$$

In order to examine the predictions of this model for the effects of bond affinity change on specific adhesion strength, Eq. 6 can be fit to our experimental data in Fig. 8. We measured N_L in our system to be $3.5 \times 10^{12} \pm 0.5 \times 10^{12}$ #/cm^2 by radioactive ligand experiments. After substitution of the constants ($k_B = 1.38 \times 10^{-23}$ J/K, $\theta = 298$ K, and $N_L = 3.5 \times 10^{12}$ molecules/cm^2) and the values for the equilibrium dissociation constant and the slope, the unknown parameters are the conversion factor η and the bond stretch l_b. A weighted least-squares two-parameter curve fit of Eq. 6 to the data is shown in Fig. 8. The fit specifies η as 1.3×10^{18} #-liter/cm^2-mol and l_b equal to 8.8 Å. (This implies that a solution/surface K_D value of 10^{-6} M, for instance, would correspond to a surface/surface value of approximately 1×10^{12} #/cm^2.) The resulting fit is shown in Fig. 8. It is replotted on logarithmic scale in Fig. 9, reinforcing the observation displayed in Figs. 3 and 7, that bond chemical affinity and mechanical adhesion strength are directly related. Moreover, a dependence of adhesion strength on the logarithm of the bond affinity is clearly exhibited.

Our covalent linkage methods permit heterogeneous coupling of the proteins to the bead and glass surfaces. It is conceivable that the effective ligand density might vary for the different IgG species, if higher affinity species are able to "see" binding sites not accessible to lower affinity species. By performing experiments to measure the amount of bound antibodies for three different species or buffer conditions, we can determine the effect of this variation of binding site availability. Using radioactive antibodies, we measured the density of bound antibodies to SpA-coated glass plates, and subsequently used these values for functional ligand density N_L. We measured active N_L for rabbit at both buffer pH 3.0 and 7.4 and for mouse at pH 7.4. The experiment gave $1.1 \times 10^{12} \pm 0.3 \times 10^{12}$ molecules/cm^2 for the number of bound rabbit antibodies at pH 7.4 buffer conditions. The identical experiment, but using pH 3.0 PBS buffer, gave a density of $1.1 \times 10^{12} \pm 0.1 \times 10^{12}$ molecules/cm^2 for the number of bound rabbit antibodies. Radiolabeled mouse IgG gave a result of $4.7 \times 10^{11} \pm 0.7 \times 10^{11}$ molecules/cm^2.

The experimental adhesion strengths for these three systems were then plotted as a function of K_D/N_L, using the functional N_L obtained from the radiolabeled experiments. Fig. 10 shows the data. The Dembo/Evans relation (Eq. 6) can be modified and fit to the data, now as a function of

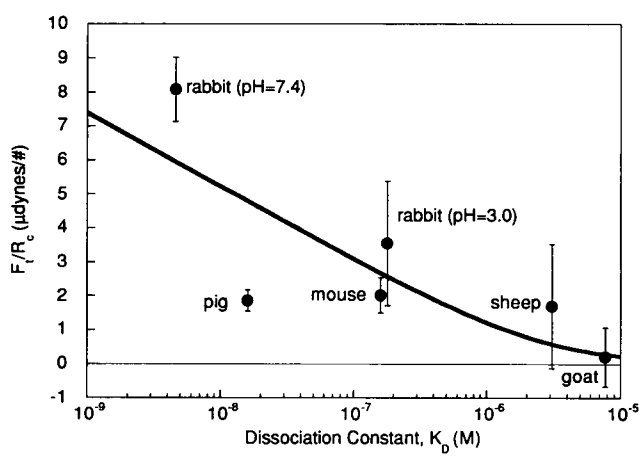

FIGURE 9 Adhesion strength per receptor present in the contact region (F_t/R_c) for the various animal species IgG, replotted as a function of dissociation constant on a logarithmic scale. The model prediction for the average bond strength is shown by the solid line.

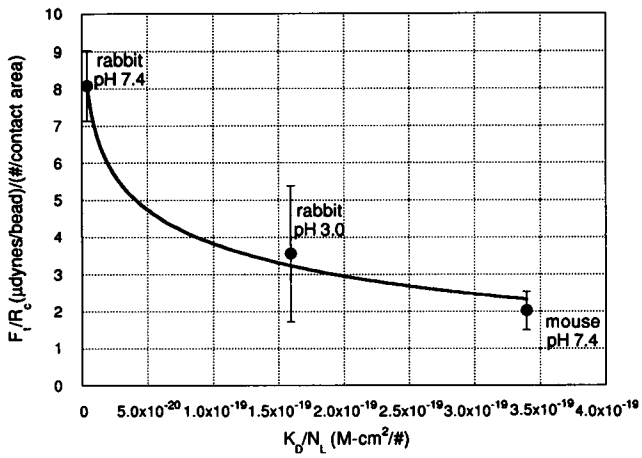

FIGURE 10 Adhesion strength per receptor present in the contact region (F_t/R_c) for the various animal species IgG, as a function of the ratio of dissociation constant to functional ligand density, K_D/N_L. Ligand densities for three different systems were measured by radiolabeled experiments. A weighted least-squares curve fit of the Dembo/Evans expression for the average bond strength, modified by the parameter η as in Eq. 6, to the data as a function of K_D/N_L, specifies $\eta = 6.7 \times 10^{17}$ #-liter/cm²-mol and l_b = 5.9 Å. The fit is characterized by $\chi^2 = 0.2$ and $R = 0.99$.

K_D/N_L. The two-parameter curve fit to the data, shown in Fig. 10, specifies $\eta = 6.7 \times 10^{17}$ #-liter/cm²-mol and l_b = 5.9 Å. All species are plotted in Fig. 11, along with the model values calculated using the parameters obtained for η and l_b in the three-point curve fit. As with the fit using constant ligand density, the model describes the experimental data quite well, using the varying values for ligand density.

An assumption underlying application of Eq. 6 to our data is that the numbers of bonds initially present before detachment begins are identical despite the K_D changes. We have so far assumed that all receptors in the contact area are bound during incubation before detachment, because the substratum ligand density (3.5×10^{12} #/cm²) is significantly larger than the two-dimensional surface K_D values under all conditions studied here and greater than all cell receptor numbers used. However, we can be more rigorous and analyze these data without this assumption. By applying an equilibrium isotherm, the expected bond number in the contact region, B_i, can be determined using the ligand density and the now-specified dissociation constant ηK_D:

$$\frac{B_i}{R_c} = \frac{N_L}{\eta K_D + N_L} \tag{7}$$

where R_c is the receptor number per bead in the contact region. We can now estimate the required detachment force *per bond* initially present. Table 2 displays the experimental specific force per bead F_t over a range of dissociation constants, using the parameters for η and l_b from the constant ligand density fits of the Dembo/Evans relation to the data. Using Eq. 6 (the curve in Fig. 9), we can determine this total force, choosing a typical receptor number of 10^6 receptors/bead or roughly 2,000 receptors in the contact area. Table 2 also displays the number of bonds, B_i, in the contact area, determined from Eq. 7, using a contact radius of 0.45 μm for a bead of 10-μm diameter, with $\eta = 1.3 \times 10^{18}$ #-liter/cm²-mol. If we assume that all bonds in the contact area are equally stressed, we can calculate a minimum force per bond. Alternatively, we can calculate a maximum force per bond by assuming that stress acts only on bonds at the contact area perimeter. Both sets of values are shown in Table 2 for comparison.

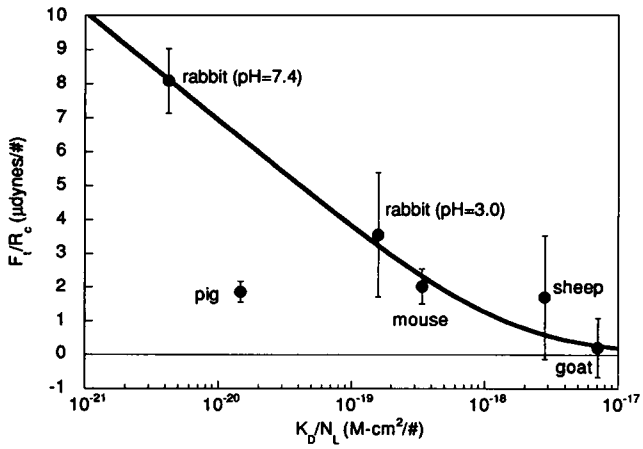

FIGURE 11 Adhesion strength per receptor present in the contact region (F_t/R_c) for the various animal species IgG, replotted as a function of K_D/N_L on a logarithmic scale. The model prediction for the average bond strength is shown by the solid line.

DISCUSSION

Mechanical strength of specific cell adhesion is generally presumed to be related to the receptor/ligand bond affinity. Theoretical models exist that predict a logarithmic dependence of mechanical detachment force on chemical affinity (Bell, 1978; Dembo et al., 1988), but no data have been previously obtained to experimentally test these models. This is the goal of our present work.

TABLE 2 Estimated force per bond for various K_D values*

K_D (M)	F_t (μdynes)	B_i	Minimum F_t/B_i (μdynes)	Maximum F_t/B_i (μdynes)
10^{-9}	15,000	2,000	7.4	330
10^{-8}	10,600	2,000	5.3	240
10^{-7}	6,300	1,950	3.2	140
10^{-6}	2,500	1,470	1.7	64
10^{-5}	400	420	1.1	22

* Specific force required per bond for bead detachment can be estimated as a function of solution/surface dissociation constant, K_D. Adhesion strengths per bond (F_t/B_i) for a range of K_D values are calculated here for two limiting cases: (1) a minimum bond force is estimated by assuming that the force on the bead acts equally on all bonds in the contact area; (2) a maximum bond force is estimated by assuming that the force on the bead acts only on the bonds at the contact area perimeter. In this table F_t is the experimental specific detachment force per bead, obtained by multiplying the values from the curve in Fig. 9 (Eq. 6) by a contact area receptor number of about 2000, as determined from a typical receptor number of 10^6 molecules/bead. The contact radius is set at 0.45 μm for a bead of 10-μm diameter. The number of contact area bonds, B_i, is obtained by using Eq. 7, with $\eta = 1.3 \times 10^{18}$ #-liter/cm²-mol. The number of perimeter bonds is estimated simply by taking the square root of B_i.

We have shown that the adhesion strength can be measured as a function of affinity, using a radial-flow detachment assay. Choosing a simple model cell system has enabled us to examine the different contributions to the adhesion process. By using latex polystyrene beads possessing well-characterized properties, many complications arising from using real cells have been minimized. The beads allow easy and systematic manipulation of the type and number of proteins on the surface. Measurement of adhesion strength over a range of receptor numbers is essential for elucidating the specific contribution of receptor/ligand bonds to overall adhesion strength, relative to nonspecific colloidal forces. Further, covalent linkage of the proteins to the bead and glass surfaces prevents alternative modes for disruption of attachment. Flow cytometric and radioactive techniques were used to measure the equilibrium dissociation constant, K_D, between IgG and SpA. Most importantly, alteration of medium pH or use of different animal species as IgG sources permitted variation of K_D over 3 orders of magnitude.

As shown in Fig. 7, the specific adhesion strength was shown to be related to the equilibrium dissociation constant, with a lower dissociation constant (greater bond affinity) corresponding to a higher slope (greater adhesion strength). These data are the very first that experimentally demonstrate a dependence of adhesion strength on receptor/ligand binding affinity. We examined these experimental results in terms of a theoretical relation combining analyses by Dembo et al. (1988) and Evans (1985). This relation predicts a logarithmic dependence of adhesion strength on bond affinity. As seen in Figs. 9 and 11, our data are essentially in accord with this prediction.

Using experimental information on bead size and contact area, we are able to estimate an average detachment force required per bond within the contact region. Depending on whether we assume that bonds are equally stressed over the entire contact area or only at the contact perimeter, we can calculate extreme of the bond force. Magnitudes of this deduced "bond strength" fall in the range of a few to a few hundred microdynes, depending on the stress assumption, as shown in Table 2. Previous theoretical (Bell, 1978) and experimental (Evans et al., 1991) estimates have given values at the lower end of this range. An interesting point to note is that Evans et al. found detachment strengths to all fall within a factor of two despite using receptor/ligand pairs that might have possessed significantly different affinities. In that particular experimental system, this observation was shown to arise from disruption of attachments by distraction of proteins from cell membrane instead of by dissociation of protein/protein bonds. Our results suggest a plausible alternative, since bond strength appears to depend only weakly on the bond affinity, in logarithmic manner. Although K_D values were not explicitly measured by Evans et al., Eqs. 6 and 7 predict that only small differences in bond strengths might have arisen from affinities differing by a couple orders of magnitude. The fact that our estimated bond strengths are greater than the force needed to extract receptors from a membrane—in the absence of cytoskeletal linkages—is consistent, however, with a likelihood of cell detachment by receptor extraction when they are not cytoskeletally linked and by receptor/ligand dissociation when they are cytoskeletally linked.

The variation of adhesion strength with bond affinity has two components contributing to it. First, the actual number of receptor/ligand bonds present in the contact region depends on the value of K_D, following Eq. 7. Second, the force required to dissociate a bond appears to increase with increasing affinity, as seen in the right-most columns of Table 2. Together, these two factors give rise to the overall increase of adhesion strength with bond affinity. Note as an example from Table 2 that the overall adhesion strength increases by a factor of about 6 for a decrease in K_D from micromolar to nanomolar range. This result depends on the ligand density, N_L, as can be seen in Eqs. 6 and 7.

A conversion factor is required to change dissociation constants measured in solution to "two-dimensional" or surface/surface dissociation constants. We are aware of no straightforward experimental technique to measure this conversion factor, but it can be deduced by matching a particular form of adhesion theory, such as the Dembo et al. model, to adhesion strength data. We have estimated the conversion factor η by fitting this model to our adhesion data to determine values for the unknowns, η and l_b. We can compare these curve-fit estimates with theoretical values. The conversion for dissociation constants can be calculated theoretically by using the gap height between the cell membrane and the surface, at closest proximity. Using a gap height of 200 Å and Avagadro's number, we obtain a theoretical value for η of 1.2×10^{15} #-liter/cm^2-mol. Comparing the theoretical value for η to the value obtained by fitting Dembo's model to the experimental data, we obtain a difference of 10^3. The higher value for the experimentally deduced conversion factor can plausibly be attributed to an effect of immobilization of the proteins, beyond mere geometry. This could be caused by the random orientation of the proteins immobilized on the surfaces, with many orientations precluding productive binding. Covalent coupling occurs through amine groups on the proteins, and all the proteins used have numerous amine groups throughout the protein structure. Multivalent interactions existing between antibodies and protein A could also contribute to the value of η, as we have assumed simple monovalent binding. For the effective bond length l_b we obtained values close to 10 Å from the model fit to the data. This estimate agrees well with expected values (Bell et al., 1984).

Some issues need to be considered carefully for future attempts to rigorously apply more detailed theoretical models to our experimental data. More complete information concerning bond stress distribution is clearly necessary. In addition, a fuller understanding of the biochemical aspects of the system, the protein-protein interactions and orientations, would be useful in drawing a conclusion about the relationship of absolute bond strengths and bond affinity. We could also improve the fit of the Dembo et al. model by using higher order terms with nonzero peeling velocities to account for

transient experimental conditions. For example, the bond association and dissociation rate constants might be incorporated, since our detachment experiments do not represent equilibrium conditions. It is possible that kinetic deviations could explain the discrepancy found for pig IgG (see Figs. 9 and 11). Nonetheless, we anticipate that analyses based on computer simulations such as that presented by Hammer and Apte (1992) should be very useful in more complete interpretation of our data.

One important application of the results is to the analysis of affinity-based cell separation processes. An example is the widely used avidin/biotin system utilized by cell affinity chromatography columns (Berenson et al., 1986). The affinity between the protein avidin and the vitamin biotin is reported to be 10^{15} liters/mol (Green, 1963) compared to the SpA/IgG association equilibrium constant on the order of 10^{8} liters/mol. Although the affinity for avidin/biotin increases by 6–7 orders of magnitude, adhesion strength on a per bond basis (as determined by Dembo's model) increases by only a factor of 2–3 greater than an ordinary bond for typical substratum ligand densities. An implication is that the adhesion bond strengths are not highly dependent on the affinities, explaining the easy removal of biotinylated cells from an avidin-coated surface by mechanical agitation (Berenson et al., 1986). Therefore, the comparative advantage of avidin/biotin chemistry to facilitate cell attachment during continuous fluid shear (Berenson et al., 1986) might in fact be due more to its unusually fast association rate constant. Such a situation would be consistent with previous theoretical (Hammer and Lauffenburger, 1987) and experimental (Lawrence and Springer, 1991) suggestions.

This work was partially supported by a grant from CellPro, Inc.
Helpful discussions with Dr. Dale Peterson and Prof. Daniel Hammer are gratefully acknowledged, as is technical assistance from Julie Auger of the University of Illinois Biotechnology Center for flow cytometry work, Gail Sudlow for protein iodination, Christine Schmidt for IRM studies, and Bruce Bromberek, Gina Ritschel, and Szu Wang for detachment experiments.

REFERENCES

Adamson, A. W. 1982. Physical Chemistry of Surfaces. 4th Ed. John Wiley & Sons, New York.

Bell, G. I. 1978. Models for the specific adhesion of cells to cells. *Science (Washington, DC)*. 200:618–627.

Bell, G. I., M. Dembo, and P. Bongrand. 1984. Cell adhesion: Competition between nonspecific repulsion and specific binding. *Biophys. J.* 45: 1051–1064.

Berenson, R. J., W. I. Bensinger, and D. Kalamasz. 1986. Positive selection of viable cell populations using avidin-biotin immunoadsorption. *J. Immunol. Methods.* 91:11–19.

Cozens-Roberts, C., J. A. Quinn, and D. A. Lauffenburger. 1990. Receptor-mediated adhesion phenomena: Model studies with the radial-flow detachment assay. *Biophys. J.* 58:107–125.

Dembo, M., D. C. Torney, K. Saxman, and D. Hammer. 1988. The reaction-limited kinetics of membrane-to-surface adhesion and detachment. *Proc. R. Soc. Lond. Ser. B* 234:55–83.

DiMilla, P., K. Barbee, and D. A. Lauffenburger. 1991. Mathematical model for the effects of adhesion and mechanics on cell migration speed. *Biophys. J.* 60:15–37.

Evans, E. 1985. Detailed mechanics of membrane–membrane adhesion and separation. I. Continuum of molecular cross-bridges. *Biophys. J.* 48: 175–183.

Evans, E., D. Berk, and A. Leung. 1991. Detachment of agglutinin-bonded red blood cells. I. Forces to rupture molecular-point attachments. *Biophys. J.* 59:838–848.

Goldman, A. J., R. G. Cox, and H. Brenner. 1967. Slow viscous motion of a sphere parallel to a plane wall. II. Couette flow. *Chem. Eng. Sci.* 22: 653–660.

Goodfriend, T. L., L. Levine, and G. D. Fasman. 1964. Antibodies to bradykinin and angiotensin: A use of carbodiimides in immunology. *Science.* 144:1344–1346.

Green, N. M. 1963. Avidin: 1. The use of [^{14}C]biotin for kinetic studies and for assay. *Biochem. J.* 89:585–599.

Hammer, D. A., and D. A. Lauffenburger. 1987. A dynamical model for receptor-mediated cell adhesion to surfaces. *Biophys. J.* 52:475–487.

Hammer, D. A., and S. A. Apte. 1992. Simulation of cell rolling and adhesion on surfaces in shear flow: General results and analysis of selectin-mediated neutrophil adhesion. *Biophys. J.* 63:35–57.

Kuo, S. C. 1992. Relationship of receptor/ligand binding parameters to model cell adhesion under fluid flow conditions. MS thesis. University of Illinois at Urbana-Champaign.

Langone, J. J. 1982a. Protein A of *Staphylococcus aureus* and related immunoglobulin receptors produced by streptococci and pneumonococci. *Adv. Immunol.* 32:157–252.

Langone, J. J. 1982b. Applications of immobilized protein A in immunochemical techniques. *J. Immunol. Methods.* 55:277–296.

Lawrence, M. B., and T. A. Springer. 1991. Leukocytes roll on a selectin at physiologic flow rates: Distinction from and prerequisite for adhesion through integrins. *Cell.* 65:859–873.

Markwell, M. 1982. A new solid-state reagent to iodinate proteins: I. Conditions for the efficient labeling of antiserum. *Analytical Biochem.* 125: 427–432.

Pharmacia. 1992. Kinetic effects of alterations in the Z-domain polypeptide derived from staphylococcal protein A. Pharmacia Biosensor Application Note, Note 303.

Saterbak, A., S. C. Kuo, and D. A. Lauffenburger. 1993. Heterogeneity and probabilistic binding contributions to receptor-mediated cell detachment kinetics. *Biophys. J.* 65:243–252.

Sharma, S. K., and P. P. Mahendroo. 1980. Affinity chromatography of cells and cell membranes. *J. Chromatogr.* 184:471–499.

Springer, T. A. 1990. Adhesion receptors in the immune system. *Nature (Lond.).* 346:425–434.

Weetal, H. H. 1976. Covalent coupling methods for inorganic support materials. *Methods Enzymol.* 44:134–148.